

# Dynamic visual stimulus presentation in an adaptive optics scanning laser ophthalmoscope

Siddharth Poonja<sup>1</sup>, Saamil Patel<sup>2</sup>, Luis Henry<sup>3</sup>, Austin Roorda<sup>1\*</sup>

1. University of California, Berkeley School of Optometry, Berkeley CA 94720-2020

2. University of Houston, Colleges of Engineering and Optometry, Center for Neuroimaging and Cognitive Science, Houston TX, 77204-2020

3. Monroe Community College, Rochester, NY, 14623

## Corresponding author:

Austin Roorda

University of California, Berkeley School of Optometry

Berkeley CA 94720-2020

Tel: 510-642-2380

Fax: 510-643-5109

Email: aroorda@berkeley.edu

\*Austin Roorda is the sole inventor on a patent that describes the concept of laser modulation in an adaptive optics scanning laser ophthalmoscope.

## Abstract

The adaptive optics scanning laser ophthalmoscope (AOSLO) has been modified to include synchronized laser modulation, making it possible to deliver adaptive optics (AO) corrected stimuli to the retina of a living eye and to record the precise retinal location where the stimulus has landed. The modification involves the development of custom software to control a high frequency pixel clock and a waveform generator board in synchrony with the scanning mirrors. The final result is a system that can project stimuli at a frame rate of 30 Hz with high sampling resolution (7.5 seconds of arc), thereby limiting the quality of the retinal image to the level of AO-correction. To demonstrate the system we show how visual acuity, as measured by a tumbling E test, is improved with aberration correction in a 5.89 mm pupil.

## 1. Introduction

The use of laser modulation to write patterns directly onto the retina while simultaneously recording them as part of the retinal image in an scanning laser ophthalmoscope (SLO) was conceived at the time of its invention by Webb et al<sup>1,2</sup>. Since that time many of the applications that were proposed have been demonstrated<sup>3</sup>, such as the ability to locate scotomas with microperimetry<sup>4</sup>, find the preferred retinal locus in eyes with central scotomas<sup>5,6</sup>, measure visual acuity (VA)<sup>3</sup> and other functional tests<sup>7</sup>, measure fixation dynamics during reading tasks<sup>8</sup>, investigate fixation in patients with retinal pathology<sup>9</sup> or reading disabilities<sup>10</sup>.

While the effectiveness of these applications are evident, the scope of the applications to date has been limited by the resolution of the eye, the size of the scan, and the sampling (pixel) density. For example, at best, a commercial SLO operates with 512 pixels over a 5 degree field. Under these conditions each pixel spans about 0.6 minutes of arc, making it difficult to generate high fidelity letters that are 20/20 (5 minutes of arc) or smaller. Furthermore, coarse pixel sampling, distortion of frames due to eye movements<sup>11</sup>, and compromised image quality (either from diffraction or aberrations) result in uncertainties in the ability to localize the position of the stimuli on the mosaic to finer than the dimension of a cone.

The adaptive optics scanning laser ophthalmoscope (AOSLO), was designed to overcome some of these limitations<sup>12</sup>. The AOSLO uses adaptive optics (AO) to compensate the aberrations that cause blur in the retinal image. In the AOSLO, wave aberrations are corrected on the way into the eye, to generate a compact focused spot on the retina, and on the way out of the eye, to form a compact image of the focused spot on the retina at the confocal pinhole. AO had already been demonstrated to improve the quality of retinal images as well as to improve the quality of the image landing on the retina<sup>13,14</sup>. More recently, it has been shown that spots smaller than the size of single cone can be imaged onto the retina<sup>15</sup>.

In this paper, we present our work to incorporate high-frequency modulation into the AOSLO scanning beam, facilitating the presentation and recording of dynamic visual stimuli during a retinal examination. This paper covers primarily the techniques involved in presenting dynamic visual stimulus through the AOSLO. As a demonstration, we measure VA by raster scanning letters onto the retina with and without adaptive optics.

## 2. Methods

### 2.1 System Parameters

The raster scan of the AOSLO is achieved by synchronous scanning of a 16 KHz horizontal resonant scan mirror and a 30 Hz vertical scan mirror. A single cycle of the vertical scan mirror encompasses 525 horizontal scan lines to form a single frame. In order to achieve the fastest scanning frequency for our system we chose the resonant scanning mirror, which has two disadvantages. First, it scans with a sinusoidal velocity profile, coming to a stop at the edges of the scan and scanning fastest through the center. Second, the scan is bidirectional while the frame grabber prefers to digitize pixels in a single direction only. To overcome these limitations, we limited our detected signal to the forward scanning segment only and limited the extent of the scan to the central 80% of the field, where the scanning velocity was most linear (The edges of the scanned field have a scan velocity that drops to about 30% that of the center of the field). Therefore, signal detection comprises only 40% of the duty cycle of the scan. Fig. 1 shows a rotated sine wave illustrating the progression of the fast-scan mirror in unison with the vertical movement of the slow-scan mirror. At the beginning of every horizontal scan, the driver control for the fast-scan mirror produces a short digital (TTL compatible) *hsync* pulse which serves as the master timer for the system. Upon each *hsync* pulse, the frame grabber is programmed to sample the detected light scattered from the retina at 20.48 MHz for 512 pixels per line. Thus, the images are sampled at 512 x 525 pixels. A photomultiplier tube (H7422-20, Hamamatsu, Japan) collects the light that reflects back from the eye to generate the analog light signal which is fed into the frame grabber.

## 2.2 AOSLO Laser Modulation Unit

Since only 40% of the scan cycle is used to record the retinal image, it is sensible to limit the light exposure to only that portion of the scan cycle in order to keep retinal exposure to a minimum. This is achieved by turning off the laser in the remainder of the scan cycle and is the most basic application for laser modulation. The system described below allows for modulation of the laser for each pixel of the image.

An amplitude-modulated Acousto-Optic Modulator, or AOM (Brimrose Corp, Baltimore, MD) is placed in the path of the laser beam serving to either deflect the laser beam into or outside the AOSLO system and hence behaving as a switch that either turns the laser beam on or off. With our current AOM, the stimuli are effectively 1 bit, since the laser can only be either ON or OFF. The switching frequency of the AOM used in the AOSLO is 50 MHz, which is sufficiently higher than the sampling rate of the frame-grabber to ensure pixel-level control of the stimulus modulation. The AOM accepts a TTL modulation signal which switches on the laser whenever it is high. The modulation signal is produced by a combination of two PCI cards, a pattern generator board UF6021 (Strategic Test Inc., Sweden) and a counter/timer board PCI-6602 (National Instruments).

The UF6021 can either use its own clock or an external clock to generate a signal encoding the pattern stored in its memory. It can either use its on-board memory (Standard Mode) or memory on a computer (FIFO Mode) to store patterns. For the purposes of producing a continuous modulation signal for the AOM in the AOSLO, we use the UF6021 in the FIFO Mode with an external clock timer. In the FIFO mode, a ring buffer of 16 buffers allocated on computer memory is used and new patterns can constantly be added to these buffers thereby permitting retinal stimulation with arbitrary dynamic stimuli of virtually infinite duration (for an animation, for example). Direct Memory Access transfers are used between the ring buffer and the UF6021 so as to transfer patterns from computer memory to on-board memory. There is minimal usage of the computer's CPU as DMA transfers enable the computer system memory to transfer data to external devices without the intervention of the CPU making the fast data transfer process very efficient.

The PCI-6602 serves as an external clock for the UF6021 and can be programmed to generate clock pulses when triggered. The *hsync* from the AOSLO is used to trigger the PCI-6602. Upon receiving each *hsync* trigger, the PCI-6602 produces a series of clock pulses, equal to the number of pixels in a line, at a frequency equal to the sampling frequency of the frame grabber (20.48 MHz). Upon each clock pulse, the UF6021 outputs a single sample from its memory corresponding to the value of the next pixel in the frame buffer. The value of this sample determines the laser modulation for the next pixel in the frame buffer. Using the *hsync* as the master timer for the PCI-6602 ensures the spatio-temporal synchronization of the modulation signal for the AOM and the sampling window of the frame-grabber.

## 2.3 Modulation of the Raster Scan

The modulation signal encodes the visual stimulus to be delivered on the raster. To better understand how raster modulation works, an example involving the presentation of a 'cross' pattern on the raster is illustrated in Fig. 1. We use the 'cross' as an example because it is a simple stimulus pattern making it easier to demonstrate the technique through a visual. The stimulus is presented within the linear portion of the sinusoidal horizontal scan. As mentioned before, a single raster scan is composed of 525 lines which form a frame. A modulation signal representing the stimulus over all the 525 horizontal lines is fed to the AOM to produce the stimulus over the raster.

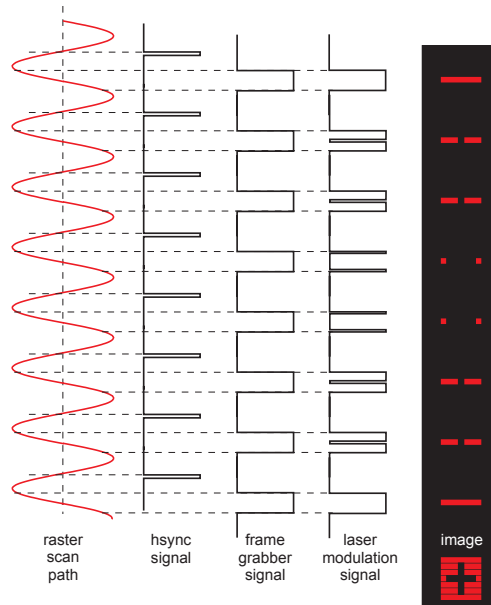


Figure 1: Simplified sequence of signals that are used to generate an image in the raster. The left column shows the path of the focused spot in the raster scan. Each time the scan mirror crosses the midpoint on the backward direction, an *hsync* pulse is generated, which serves as the master timer for the entire AOSLO system. The *hsync* signal is used to trigger the line-by-line acquisition of the image by the frame grabber and is shown as the third trace in the figure. The frame grabber signal shows that the image acquisition occurs in the linear portion of the scanning spot in the forward direction. The laser modulation and the frame grabber are synchronized by a common *hsync*. The last column shows the light pattern falling on the retina for the corresponding line scan. In the first line, the frame grabber simply turns the laser on and off at the beginning and end of the line. In the second scan line, the modulation briefly switches the AOM off to produce a line on the retina with a dark cut in the middle. The laser modulation in the subsequent lines of the frame is performed similarly to produce the 'cross' image.

## 2.4 What is seen by the subject?

The subject sees the raster and stimulus as they are blurred by the residual aberrations in the instrument/eye system, in other words, the raster containing the stimulus is convolved with the aberrations of the eye and optical system. Without adaptive optics, the raster appears as a normally-blurred distant object. When the adaptive optics is activated, the raster along with the stimulus becomes very sharp.

## 2.5 What is recorded in the AOSLO image?

The AOSLO records an image that is a product of the retinal image with the delivered stimulus. Therefore, the stimulus as seen on the AOSLO image does not reflect how the subject sees it. Even when the aberrations are not corrected and the retinal image is blurred, the stimulus still appears on the AOSLO image with 100% contrast. This feature is unique to scanning systems and it arises because of the temporal nature of the scan. During the time that the laser is turned off it is necessary that the pixels acquired during that time will be dark. Conversely, when the laser is on, each pixel will be sampled normally. Nonetheless, the location of the stimulus on the retinal image indicates exactly where the image has landed on the retina; there is no artifact.

## 2.6 System Testing

To demonstrate the technology and to also underline the benefits of AO, we measured VA over a 5.89 mm pupil before and after correcting the aberrations with AO. Six subjects between the ages of 20 and 41 with normal ocular health were recruited for the study. This research followed the tenets of the World Medical Association Declaration of Helsinki. Informed consent was obtained from the subjects after we explained the nature and possible complications of the study. The experiment was performed at the University of Houston College of Optometry and it was approved by the University of Houston Committee for the Protection of Human Subjects.

The VA task was a four-alternative-forced-choice tumbling 'E' test. The stimulus was the letter 'E' presented in one of four different orientations (Fig. 3). Letter sizes were presented in random order for seven sizes ranging linearly in angular subtense from 1.25 to 5 minutes of arc (20/5 to 20/20). Each stimulus was presented continuously and for as long as the subject required to make a response, after which point the new stimulus was displayed. Ten presentations were made for each letter size at each orientation for a total of 280 trials. The data were plotted as the percentage of correct responses vs letter size and were fitted with a base-e Weibull psychometric function. The threshold which we used to determine VA was at 72.4% correct, which corresponds to the inflection point of the Weibull function fit.

Subjects were cyclopleged with a combination of 2.5% phenylephrine and 0.5% tropicamide about 30 minutes prior to the experiment. Once dilated and cyclopleged, subjects were aligned into the system and the initial wave aberrations were measured. To aid head alignment and stability, subjects bit into a dental impression mount, which was fixed to an X-Y-Z stage.

VA under two conditions was tested. Under both conditions the entrance beam diameter was 5.89 mm which is the maximum beam diameter of the AOSLO system. The first condition was VA without high-order aberration correction. Under this condition, defocus and astigmatism were corrected in the eye to less than 0.25 diopters, based on the root-mean-squared (RMS) wave aberration that was measured while the eye was aligned in the system. Since RMS-based measurements are known not to provide accurate assessments of refraction<sup>16;17</sup> we allowed each subject to adjust the defocus to their preferred level before starting the procedure. Defocus was adjusted by adding spherical curvature to the deformable mirror in the light path. With guidance from the AOSLO operator, the subject was able to make a fine defocus adjustment ( $\pm 0.1$  D) to find their preferred focal plane. Under the no-AO condition, the typical RMS wave aberration for high orders was about 0.5 micrometers which included the residual defocus and astigmatism. After the subjects chose their preferred focal plane, the RMS values were generally higher. The second condition was VA with high-order aberration correction. Under this condition, the AO system was continuously run to measure and compensate the aberrations of the eye to a minimum level. Typical RMS wave aberration levels were kept at 0.1 micrometers or lower during the task. Image quality was monitored continuously during the experiment. Since it was presumed that after AO-correction, the image plane corresponded to the preferred image plane, the subjects were not permitted to make any focus adjustment in this condition. For both conditions, the patient was allowed to sit out of the system and relax whenever they wanted to. For the AO-corrected condition, whenever the image quality or level of correction noticeably degraded the patient was asked to sit out.

For each trial, the subject indicated the orientation of the 'E' using a joystick. The responses were recorded along with short video segments for each trial which contained the retinal image along with the delivered stimulus. After 280 trials, the data were analyzed to compute the VA.

## 2.7 Field size calibration:

As stated above, the horizontal scanner has a sinusoidal velocity profile, whereas the frame grabber acquires pixels at a fixed frequency. As a result, pixels across the center of each scan line span relatively less retinal horizontal space than pixels toward the edges. The result is an image that is distorted in the horizontal direction, appearing to be stretched at the edges. Consequently, if a stimulus presented to the retina appears undistorted in the buffer containing the encoded stimulus for laser modulation, it will appear distorted on the retina, in this case appearing more compressed at the edges in the horizontal direction. In order to set the image, or parts of the image, to a specific field size, we constructed a model eye with a retina that was comprised of a grid with 0.1 degree squares. The amplitudes of the scan mirrors were set until the desired number of squares were visible in the image.

For this experiment, it was necessary to have calibrated pixel dimensions only in the center of the frame where the stimulus was presented. Since the central region of the scan was effectively linear, we adjusted the scan angles so that a 0.1 degree square region in the center of the frame spanned 48 X 48 pixels. Under this setting, the scan velocity over the extent of the stimulus was linear to within 2% and the pixel sampling dimensions were 7.5 X 7.5 seconds of arc. The small pixel size made it possible to generate precise letter sizes in the stimulus. For example, the 20/5 letter 'E' was 10 X 10 pixels (1.25 minutes of arc) and the 20/20 letter was 40 X 40 pixels (5 minutes of arc).

## 3.0 Results

Figure 2 shows an example of an image acquired with the stimulus delivery activated. A summary of the VA results from all subjects is shown on figure 3. The absolute VA levels were variable, but the results clearly show a marked improvement in VA after aberration correction. The reduction in the minimum angle of resolution was 33% (two tailed T-test,  $p < 0.001$ ).

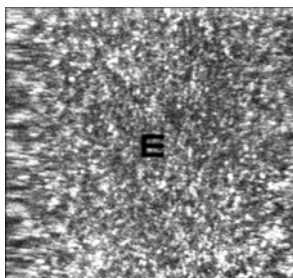


Figure 2: The image is a single unprocessed frame from a video of the fovea of subject LH. I also shows the 20/20 letter 'E' projected that was projected onto the retina at that time. The letter spans 40 pixels. The sinusoidal scan causes the field distortion which gives rise to the horizontal stretch in the unprocessed frame.

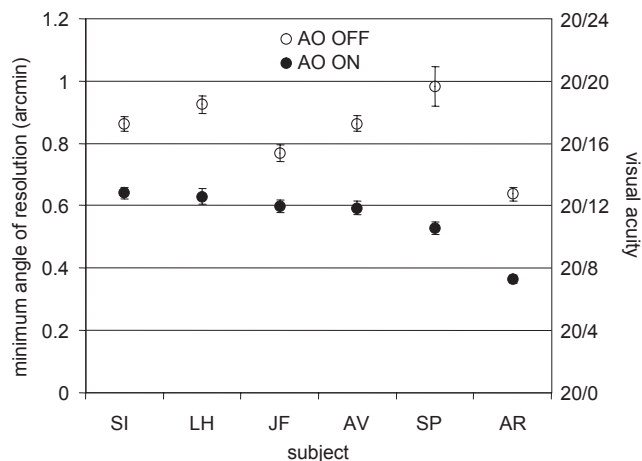


Figure 3: Improvement in VA with adaptive optics. The open circles represent the VA for a 5.89 mm pupil without AO-correction. The solid circles represent the VA with AO correction. The average improvement in resolution is 33% after correction of high-order aberrations.

#### 4.0 Discussion

This is the first demonstration of an instrument that can project an AO-corrected stimuli onto the retina while simultaneously recording its location. Although the technique of stimulus presentation and recording is not new, the combination of AO and the small field size bring the technique to a microscopic level. In this paper, we demonstrated a rather simple experiment where VA was measured with and without AO. Our results showed a significant improvement in vision after aberration correction, but none except one subject reached the theoretical limits of about 20/8 imposed by the photoreceptor mosaic<sup>18</sup>. It should be noted that subject AR had spent more time as a subject in the system than any of the other subjects, so the improved performance might reflect a training effect, or familiarity with the system.

Our subjects performed much better than those in a similar study done by Yoon and Williams<sup>14</sup>. The main differences between the Yoon and Williams study and ours were (i) their subjects viewed a CRT monitor through an AO system, (ii) they used a higher threshold for determining VA (80% vs 74.2%) (iii) they used a 6 mm pupil and we used a 5.89 mm pupil and (iv) their stimulus had lower illuminance (1.76 logTd vs 6.1 logTd). Regarding difference (i), uncorrected aberrations in their independent display channel might account for a lower VA. Regarding difference (ii), a change in threshold from 72.4% to 80% only accounts for about a 7% drop in acuity for our subjects, which can explain only a fraction of the difference in VA. The decreased diffraction caused by difference (iii) would, if anything, slightly improve the acuity of Yoon et al's subjects. Lower luminance (difference (iv)) remains the most plausible cause for their reports of lower acuity.

Although we presented a system whereby the recorded videos indicate the exact location of the tumbling 'E' stimulus on the retina during the VA task, that information was not used in the VA analysis. Examples of experiments that will benefit from both AO-corrected images as well as the ability to present AO-corrected stimuli include high-resolution microperimetry, investigating the role of eye movements on the eye's ability to judge apparent motion<sup>19</sup>, dynamic fixation measurements<sup>20</sup>, investigating the role of retinal sampling density on VA, and recording perceived color responses from specific individual cones in the retina<sup>15</sup>.

#### 5.0 Conclusion

We present the technical details of our modification of the Adaptive Optics Scanning Laser Ophthalmoscope whereby we project AO-corrected stimuli directly onto the retina while simultaneously recording their position on the retina. The system is demonstrated by showing how correcting the eye's monochromatic aberrations with adaptive optics can improve SLO-projected VA. Over a 5.89 mm pupil the minimum angle of resolution was reduced on average by 33%, representing a significant and meaningful VA improvement. The system has the potential to be used for many basic and clinical investigations of the eye.

#### Acknowledgements

This work was funded by the National Institutes of Health Bioengineering Research Partnership Grant EY014375 and the National Science Foundation Science and Technology Center for Adaptive Optics, managed by the University of California at Santa Cruz under cooperative agreement #AST-9876783.

## References

- (1) Webb RH, Hughes GW, Pomerantzeff O. Flying spot TV ophthalmoscope. *Appl Opt* 1980; 19:2991-2997.
- (2) Webb RH, Hughes GW. Scanning laser ophthalmoscope. *IEEE Transactions on Biomedical Engineering* 1981; 28:488-492.
- (3) Mainster MA, Timberlake GT, Webb RH, Hughes GW. Scanning laser ophthalmoscopy. Clinical applications. *Ophthalmology* 1982; 89(7):852-857.
- (4) Timberlake GT, Mainster MA, Webb RH, Hughes GW, Trempe CL. Retinal localization of scotomata by scanning laser ophthalmoscopy. *Invest Ophthalmol Vis Sci* 1982; 22(1):91-97.
- (5) Timberlake GT, Mainster MA, Peli E, Augliere RA, Essock EA, Arend LE. Reading with a macular scotoma. I. Retinal location of scotoma and fixation area. *Invest Ophthalmol Vis Sci* 1986; 27(7):1137-1147.
- (6) Guez JE, Le Gargasson JF, Rigaudiere F, O'Regan JK. Is there a systematic location for the pseudo-fovea in patients with central scotoma? *Vision Res* 1993; 33(9):1271-1279.
- (7) Guez JE, Le Gargasson JF, Massin P, Rigaudiere F, Grall Y, Gaudric A. Functional assessment of macular hole surgery by scanning laser ophthalmoscopy. *Ophthalmology* 1998; 105(4):694-699.
- (8) Timberlake GT, Peli E, Essock EA, Augliere RA. Reading with a macular scotoma. II. Retinal locus for scanning text. *Invest Ophthalmol Vis Sci* 1987; 28(8):1268-1274.
- (9) Jamara RJ, Van de velde F, Peli E. Scanning eye movements in homonymous hemianopia documented by scanning laser ophthalmoscope retinal perimetry. *Optom Vis Sci* 2003; 80(7):495-504.
- (10) MacKeben M, Trauzettel-Klosinski S, Reinhard J, Durrwachter U, Adler M, Klosinski G. Eye movement control during single-word reading in dyslexics. *J Vis* 2004; 4(5):388-402.
- (11) Stetter M, Sendtner RA, Timberlake GT. A novel method for measuring saccade profiles using the scanning laser ophthalmoscope. *Vision Res* 1996; 36(13):1987-1994.
- (12) Roorda A, Romero-Borja F, Donnelly WJ, Queener H, Hebert TJ, Campbell MCW. Adaptive optics scanning laser ophthalmoscopy. *Optics Express* 2002; 10(9):405-412.
- (13) Liang J, Williams DR, Miller D. Supernormal vision and high-resolution retinal imaging through adaptive optics. *J Opt Soc Am A* 1997; 14(11):2884-2892.
- (14) Yoon GY, Williams DR. Visual performance after correcting the monochromatic and chromatic aberrations of the eye. *J Opt Soc Am A* 2002; 19(2):266-275.
- (15) Hofer H, Singer B, Williams DR. Different sensations from cones with the same pigment. *J Vision* 2005; 5(5):444-454.
- (16) Cheng X, Bradley A, Thibos LN. Predicting subjective judgment of best focus with objective image quality metrics. *J Vis* 2004; 4(4):310-321.
- (17) Guirao A, Williams DR. A method to predict refractive errors from wave aberration data. *Optom Vis Sci* 2003; 80(1):36-42.
- (18) Williams DR. Aliasing in human foveal vision. *Vision Res* 1985; 25:195-205.
- (19) Stevenson SB, Raghunandan A, Frazier J, Poonja S, Roorda A. Fixation jitter, motion discrimination and retinal imaging. *Journal of Vision* 4[11], 85. 2004. (Abstract)
- (20) Putnam NM, Hofer H, Doble N, Chen L, Carroll J, Williams DR. The locus of fixation and the foveal cone mosaic. submitted to *J Vision* 2005.